TUNABLE Q-SWITCHED LASER USING ROSE GOLD-BASED SATURABLE ABSORBER

ADZLAN MUHAYMIN BIN IDRIS

FACULTY OF ENGINEERING
UNIVERSITY OF MALAYA
KUALA LUMPUR

2018

TUNABLE Q-SWITCHED LASER USING ROSE GOLD-BASED SATURABLE ABSORBER

ADZLAN MUHAYMIN BIN IDRIS

DISSERTATION SUBMITTED IN FULFILMENT OF THE REQUIREMENTS FOR THE DEGREE OF MASTER IN TELECOMMUNICATION ENGINEERING

FACULTY OF ENGINEERING
UNIVERSITY OF MALAYA
KUALA LUMPUR

2018

UNIVERSITY OF MALAYA

ORIGINAL LITERARY WORK DECLARATION

Name of Candidate: Adzlan Muhaymin bin Idris

(I.C/Passport No:

Matric No: KQH 160002

Name of Degree: Master of Telecommunication Engineering

Title of Project Paper/Research Report/Dissertation/Thesis ("this Work"):

Tunable Q-Switched Laser Using Rose Gold-based Saturable Absorber

Field of Study: Photonics (Electronics and Automation)

I do solemnly and sincerely declare that:

(1) I am the sole author/writer of this Work;
(2) This Work is original;
(3) Any use of any work in which copyright exists was done by way of fair dealing and for permitted purposes and any excerpt or extract from, or reference to or reproduction of any copyright work has been disclosed expressly and sufficiently and the title of the Work and its authorship have been acknowledged in this Work;
(4) I do not have any actual knowledge nor do I ought reasonably to know that the making of this work constitutes an infringement of any copyright work;
(5) I hereby assign all and every rights in the copyright to this Work to the University of Malaya ("UM"), who henceforth shall be owner of the copyright in this Work and that any reproduction or use in any form or by any means whatsoever is prohibited without the written consent of UM having been first had and obtained;
(6) I am fully aware that if in the course of making this Work I have infringed any copyright whether intentionally or otherwise, I may be subject to legal action or any other action as may be determined by UM.

Candidate's Signature Date:

Subscribed and solemnly declared before,

Witness's Signature Date:

Name:

Designation:

TUNABLE Q-SWITCHED LASER USING ROSE GOLD-BASED SATURABLE ABSORBER

ABSTRACT

In this dissertation, a tunable laser using rose-gold based saturable absorber (SA) was researched. The SA was prepared using sodium borohydrate ($NaBH_4$) reduction method by mixing Gold (III) chloride trihydrate ($HAuCl_4$) (~50% Au-based), Polysodium-4-styrenesulfonate (PSSS), tri–sodium citrate (TSC) ($Na_3C_6H_5O_7$), and $NaBH_4$. Ring cavity laser setup was deployed to generate train of pulses for optical parameters measurement. Three experiments were conducted where the output lasers were tuned to 1539.88 nm, 1550.17 nm, and 1560.21 nm wavelength. For each experiment, input pump power was increased in step of 10 mW starting from the lowest threshold power where the SA would start to act as a Q-switch. The lowest and highest thresholds were different for each output wavelength, producing different power pumping range. The recorded ranges for input pump power were 35 mW to 115 mW (1539.88 nm), 45 mW to 165 mW (1550.17 nm), and 40 mW to 170 mW (1560.21 nm). Peak output powers monitored for each laser were 1.17 mW (1539.88 nm), 2.64 mW (1550.17 nm), and 2.36 mW (1560.21 nm). Laser efficiencies were obtained by measuring the slope when plotting output power to input pump power. Obtained laser efficiency values were 1.296 % (1539.88 nm), 1.900 % (1550.17 nm), and 1.612% (1560.21 nm). It was concluded that the SA was best-suited to be paired with Erbium-doped fiber laser (EDFL) for laser generation at 1550 nm.

Keywords: tunable laser, rose gold, saturable absorber, Q-switched, laser efficiency

TUNABLE Q-SWITCHED LASER USING ROSE GOLD-BASED SATURABLE ABSORBER

ABSTRAK

Dalam disertasi ini, laser-boleh-ubah dengan menggunakan penyerap bertepu berunsurkan ros emas sebagai suis-Q telah dikaji. Penyerap bertepu telah difabrikasi melalui prosedur reduksi sodium borohydrate ($NaBH_4$) dengan mencampurkan emas (III) klorid trihidrat (~50% berunsurkan emas), Polysodium-4- styrenesulfonate (PSSS), tri–sodium sitrat (TSC) ($Na_3C_6H_5O_7$), dan $NaBH_4$. Rongga laser dalam bentuk cincin telah digunakan untuk menghasilkan deretan denyutan untuk pengukuran parameter-parameter optik. Tiga eksperiman telah dijalankan di mana keluaran laser telah ditala ke gelombang pulsa berukuran 1539.88 nm, 1550.17 nm, and 1560.21 nm. Untuk setiap eksperimen, kuasa pam input telah ditingkatkan dalam langkah 10 mW bermula daripada kuasa terendah di mana penyerap bertepu telah bertindak sebanga suis-Q. Kuasa terendah dan tertinggi adalah berbeza untuk setiap keluaran gelombang pulsa, dan ini menghasilkan julat-julat berbeza untuk kuasa pam keluaran. Julat-julat yang telah direkodkan untuk kuasa pam input adalah 35 mW ke 115 mW (1539.88 nm), 45 mW ke 165 mW (1550.17 nm), dan 40 mW ke 170 mW (1560.21 nm). Kuasa puncak keluaran yang telak disaksikan adalah 1.17 mW (1539.88 nm), 2.64 mW (1550.17 nm), dan 2.36 mW (1560.21 nm). Keefisienan laser telah diperoleh dengan mengira kecerunan apabila kuasa pam keluaran diplot kepada kuasa pam input. Nilai keefisienan laser yang dicapai adalah 1.296 % (1539.88 nm), 1.900 % (1550.17 nm), dan 1.612% (1560.21 nm). Ia telah disimpulkan bahawa penyerap bertepu adalah paling sesuai untuk dipasangkan bersama laser fiber-terdop-erbium untuk penghasilan laser pada 1550 nm.

ACKNOWLEDGEMENTS

I would like to denote my sincerest gratitude to my supervisor Prof. Dr. Sulaiman Wadi Harun for his unceasing support during the course of this research and also in my Master study. His lectures in Optical Networks and Laser Electronics have helped me to better understand the topic and his counsels have assisted me to complete this dissertation.

I would also like to thank Mr. Muhammad Farid bin Mohd Rusdi, Mr. Anas bin Abdul Latiff, Mr. Ahmad Haziq Aiman Rosol, and Ms. Umi Namirah binti Zakaria from the Photonic Research Center (PRC). The completion of this dissertation was made possible with their passionate involvement and insightful inputs throughout the experiments.

Last, but by no means least, I would like to thank my family, friends, and colleagues. Their loves and supports have helped me to get through difficult times, both in my study and life in general.

TABLE OF CONTENTS

LIST OF FIGURES

LIST OF TABLES

LIST OF SYMBOLS AND ABBREVIATIONS

°C	:	Degrees Celsius
µm	:	Micrometer
µs	:	Microsecond
a.u.	:	Arbitrary unit
Ag	:	Silver
AlGaAs	:	Aluminum gallium arsenide
AOM	:	Acousto-optic modulator
ArF	:	Argon Fluoride
Au	:	Gold
Cd	:	Cadmium
Cl	:	Chlorine
cm	:	Centimeter
CO	:	Carbon monoxide
CO_2	:	Carbon dioxide
COT	:	Cycloheptatriene and cyclooctatetraene
Cr^{3+}:Al_2O_3	:	Ruby
Cu	:	Copper
cw	:	Continuous wave
dB	:	Decibel
dB/km	:	Decibel-per-kilometer
DPS	:	Differential phase shift
EDF	:	Erbium-doped fiber
EDFL	:	Erbium-doped fiber laser
EM	:	Electromagnetic

EOM	:	Electro-optic modulator
Er	:	Erbium
Er:YAG	:	Erbium-doped yttrium aluminum garnet
F	:	Fluorine
Fe	:	Iron
FESEM	:	Field emission scanning electron microscopy
fs	:	Femtosecond
FWHM	:	Full width at half-maximum
GaAs	:	Gallium arsenide
GaN	:	Gallium nitride
GNR	:	Gold nanorode
GW	:	Gigawatt
$HAuCl_4$	:	Gold (III) chloride trihydrate
HDF	:	Holmium-doped fiber
HeNe	:	Helium neon
Ho:YAG	:	Holmium-doped yttrium aluminum garnet
Hz	:	Hertz
IoT	:	Internet of things
IR	:	Infrared
$J.K^{-1}$	:	Joule per Kelvin
J.s	:	Joule-second
K	:	Kelvin
keV	:	Kiloelectron volt
KrF	:	Krypton fluoride
kW	:	Kilowatt
LD	:	Laser Diode

LFEX	:	Laser for fast ignition experiments
LMF	:	Loop-mirror-filter
mJ	:	Millijoule
mL	:	Milliliter
mL/min	:	Milliliter per minute
mm	:	Millimeter
mm^2	:	Millimeter square
mW	:	Milliwatt
MΩ	:	Megaohm
N_2	:	Nitrogen
NA	:	Numerical Aperture
$NaBH_4$	:	Sodium borohydrate
NaCMC	:	Sodium carboxymetyl cellulose
Nd:CNGG	:	Neodymium-doped calcium niobium gallium garnet
Nd:YAG	:	Neodymium-doped yttrium aluminum garnet
$Nd:YVO_4$	:	Neodymium-doped yttrium vanadate
Ni	:	Nickel
nm	:	Nanometer
NP	:	nanoparticle
ns	:	Nanosecond
Pd	:	Palladium
PMC	:	Polarization mode converter
ps	:	picosecond
OSA	:	Optical spectrum analyzer
OSC	:	Oscilloscope
PCB	:	Printed circuit board

PSS	:	Polysodium-4- styrenesulfonate
Pt	:	Platinum
PVA	:	Polyvinyl alcohol
PW	:	Petawatt
rad	:	Radians per second
RF	:	Radio Frequency
RIN	:	Relative intensity noise
RPM	:	Revolutions-per-minute
SA	:	Saturable absorber
SM	:	Single mode
SMF	:	Single mode fiber
SNR	:	Signal-to-noise ratio
TEM	:	Transmission electron microscopy
Ti-Sapphire	:	Titanium-sapphire
TM	:	Transverse magnetic
TMD	:	Transition-metal dichalcogenides
TSC	:	Tri-sodium citrate
UV	:	Ultraviolet
VCSEL	:	Vertical-cavity surface-emitting laser
WDM	:	Wavelength division multiplexing
Xe	:	Xenon
XRD	:	X-ray diffraction
Yb	:	Ytterbium
YbAG	:	Ytterbium aluminum garnet
Zn	:	Zinc
ZrB_{12}	:	Zirconium Boride

CHAPTER 1: INTRODUCTION

1.1 Background and Research Motivation

Since laser was first conceived on May 16th, 1960 by Theodore H. Maiman (Shori, Schepler, & Clarkson, 2007), quantum leaps have been made in many scientific fields. The search for laser that would yield the highest peak power at optimum stability and reliability is still ongoing. Peak power of 2-petawatts (PWs), or 2 x 10^{15} W, was demonstrated when Osaka University, Japan fired up its Laser for Fast Ignition Experiments (LFEX) (Miyanaga & Kawanaka, 2011) back in 2015 (Sarri, 2015). Produced temperature of 5 kiloelectron-volt (keV), which translates to 58022.6 Kelvin (K) or 57749.5 degrees Celsius (°C), has allowed scientists to recreate the extreme condition of the early universe. However, the energy was sustained for only a mere one-trillionth of a second (1×10^{-12} s) or 1 picosecond (ps). Other practical use of LFEX is the study of nuclear fusion due to plasma being produced by the extreme temperatures (Krokhin, 1972).

Before we look into the extreme ends of what could be researched with lasers, academics must never forget the foundations of laser. A laser, which stands for “Light Amplification by Stimulated Emission of Radiation”, is a quantum device (Verdeyen, 1995). The study of laser is the study of interacting photons, the quanta of light. Light produced by laser is coherent, highly directional, and monochromatic. One method to produce high quality laser is Q-switching, where peak power in the range of kilowatts (kWs) to gigawatts (GWs), is generated for pulse duration in the range of nanoseconds (ns) to microseconds (µs). High pulse energies are the results of low pulse repetition, and vice versa. Recently, an active Q-switched Er:YAG laser using cavity-dumped operation as active components has achieved energy of 6 millijoules (mJ) with pulse duration of 15 ns, which equals to 400 kW of power (Ottaway, Harris, Clark, & Veitch, 2016). Alternatively, a passive Q-switch employs the use of saturable absorbers (SAs).

SAs are materials that absorb light at a rate inversely proportional to incident light intensity. Important parameters that define a good SA are broad absorption wavelength band (range of wavelength where lights are absorbed), reasonable modulation depth or slope efficiency, fast recovery time, high optical damage threshold, plus cost over time efficiency to fabricate the SA. Work done by (Gene, Kim, & Lim, 2018) showed holmium-doped fiber (HDF) with the length of 10 centimeters (cm) as a SA returned a modulation depth of 56% at wavelength of 1970 nanometers (nm) with saturated power of 20 milliwatts (mWs) for all wavelength measured.

The primary motivation for researchers investigating SAs is to discover the best materials to fabricate SAs. Since there are infinite combinations of chemical elements that can be synthesized in a lab to produce a SA, and also many types of fiber laser that the SA can be paired with, the research is ongoing everywhere. What this dissertation hopes to prove is that rose gold is a suitable selection for constructing a SA. This is due to the bandwidth of gold nanoparticles which is tunable by modifying the size of the nanoparticles (Tanahashi et al., 1996). This tunable characteristic is required in broadband photonics devices.

1.2 Objectives

The goal of this research is to establish rose gold as a reliable alternative SA. This research work is guided by the undermentioned objectives:

(i) To fabricate and characterize rose gold-based SA.

(ii) To generate tunable laser using rose gold-based SA.

(iii) To evaluate the performance of the laser and compared it to other SAs from previous works.

1.3 Research Overview

This research report is organized into five chapters, where the generation of laser using SA made of rose gold is demonstrated and investigated. The first chapter introduces the background of the topic, where the motivations behind this research and its objectives are concisely outlined.

Chapter 2 illustrates the important components needed to appreciate this report; the literature review for lasers, Q-switching techniques, SAs, the gold element, and optical parameters. Chapter 3 renders on how the tunable Q-switched laser is achieved. This includes the setup of the apparatus and materials required.

Chapter 4 presents the results of the experiments, which prove that rose gold is a viable alternative for SA. Chapter 5 summarizes the outcomes of this dissertation and puts forward recommendations for prospect works.

CHAPTER 2: LITERATURE REVIEW

2.1 Introduction

Albert Einstein's works on stimulated emission in 1916 (Foth, 2008) would later become the theoretical backbones for laser and maser (microwave amplification by stimulated emission). However, devices based on them could not have been materialized at the time due to the deficiency in technological advancement, and the terms laser and maser were only coined in 1950s. A hundred years since Einstein's paper, many types of maser and lasers have been built and researches on how to improve them are an on-going venture.

2.2 Working Principle of Laser

2.2.1 Light

There are two models to identify the properties of light (Ulaby, Michielssen, & Ravaioli, 2010). Firstly, light is treated as an electromagnetic (EM) wave. Simplest equation to describe light propagating on single plane in x-direction, E(x,t) is:

$$E(x,t) = E_0 \sin(\omega t - kx) \qquad (2.1)$$

E_0 is the amplitude of the electric field at time t, ω is the angular frequency in radians per second ($\omega = 2\pi\upsilon = 2\pi/T$), υ is the frequency of the signal in Hz, T is the period of the signal, k is the wave vector or wave number where $k = 2\pi/\lambda$, and λ is the wavelength of the travelling light measured in SI unit meter. One important equation describing the relation of frequency, υ, to wavelength λ is

$$c = \lambda\,\upsilon \qquad (2.2)$$

where c is the speed of light with the officially sanctioned value of 299,792,458 ms^{-1} (Davis, 2018).

Although the first model was sufficient to describe refraction and diffraction of light, it has been proven to be inadequate when investigating light at atomic and molecular level. For this, light has been treated as flux of photons by Einstein (Thyagarajan & Ghatak, 2010), with each photon traveling at the speed of light *c* and has the energy of

$$E = h\upsilon \tag{2.3}$$

where υ is the frequency mentioned earlier and *h* is the Planck's constant with the value $h = 6.675\text{x}10^{-31}$ Js.

2.2.2 Amplification

In electronics, amplification is the process of guiding an input signal towards an amplifier to obtain an output signal that has higher amplitude (and/or changes in other signal properties) than the input. In laser, amplification occurs inside lasing medium, also known as active laser medium or gain medium. Types of lasers are classified by the state of the lasing medium such as solid, liquid, gases, excimer, or semiconductor, which are discussed in subchapter 2.2.4.

Amplification of visible light (EM spectrum of 380 nm to 750 nm) is not as straightforward as amplifying signal in electronic circuits that has signal in micrometer (µm) to millimeter (mm) wavelength (T. H. Lee, 2004). The process for amplifying light was theorized by Einstein in his paper regarding stimulated emission.

2.2.3 Stimulated Emission

There were three optical processes brought forth by Einstein, which were (a) spontaneous emission (b) stimulated emission and (c) absorption (K.-H. Wu, 2009). The three processes are illustrated in Figure 2.1.

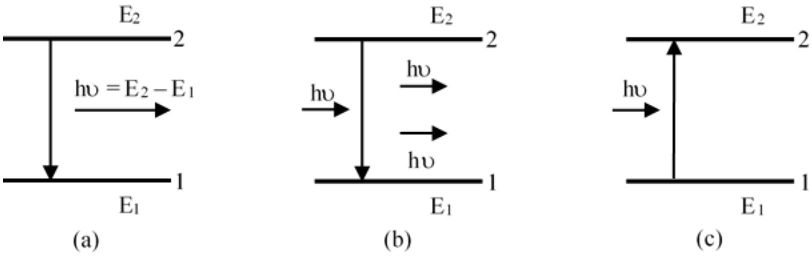

Figure 2.1: (a) Spontaneous emission (b) Stimulated emission (c) Absorption

Let 1 and 2 be the energy levels of atom, with their energies are denoted as E_1 and E_2 respectively, and $E_2 > E_1$. For the sake of convenience, Level 1 will be taken as the ground level. In (a) spontaneous emission, the atom is initially at Level 2. Higher energy level means the atom is not stable, thus it tends to decay back to ground level. Energy released in the form of EM wave during the decay process is equal to $h\upsilon = E_2 – E_1$. The frequency of the radiated wave, υ, is given by

$$\upsilon = (E_2 – E_1)/h \qquad (2.4)$$

For the case of (b) stimulated emission, incident photon with the energy of $E = h\upsilon$ has the exact atomic frequency of the incident material. Atoms in Level 2 are forced, or stimulated to decay to the ground level with finite probability. In doing so, each atom will release a photon with energy $E = h\upsilon$, which is the exact amount of energy as incident photon. It is understood from here that incident photon creates identical photon travelling in the same direction.

In (c) absorption process, atoms in ground level will remain in the same level unless stimulation is provided. A finite probability also exists for atoms in the ground level to jump to higher level when incident photon with energy $h\upsilon = E_2 – E_1$ impinges on the material and υ is equal to the atomic frequency of the material. The difference between (c) and (b) is that absorption does not result in any photon.

When *finite probability* is mentioned, it means the probability for stimulated emission to occur is small. Fundamental law of thermodynamics, embodied as Boltzmann's principle, expressed that when a group of atoms is at thermal equilibrium, the relative population of two energy levels is denoted by

$$\frac{N_2}{N_1} = \exp\left(-\frac{E_2 - E_1}{kT}\right) \qquad (2.5)$$

where N_1 and N_2 are the atoms population in Level 1 and Level 2, respectively, T is the equilibirium temperature in kelvin, and k = 1.38065 x 10^{-23} J.K^{-1} is the Boltzmann's constant (C. Townes, 2004). Using $h\upsilon = E_2 - E_1$, the difference between population,

$$\Delta \mathrm{N} = N_1 - N_2 = (1 - e^{-\frac{hv}{kT}})N_1 \qquad (2.6)$$

shows that there will be more atoms in lower level during thermal equilibrium. Thus, the atoms in incident material is going to be net absorber, not net emitter, which results in no light amplification and no emission. Accordingly, *population inversion* is a requirement to generate laser.

2.2.3.1 Population Inversion

Through Chemistry, it is known that atoms have many more energy levels with each level having their own decay time constant, τ (Hitz, Ewing, & hect, 2012). It is preferred that atoms would not return to the ground state in the shortest time. For this reason, four-level laser is considered to be the optimal, realizable laser and has found its way in many applications. A LED-pumped Nd:YAG laser with highest reported 9% optical efficiency is an example of four-level system (Huang, Su, Lin, Chiu, & Huang, 2016). Energy diagram for the four-level laser pumping system is exemplified in Figure 2.2.

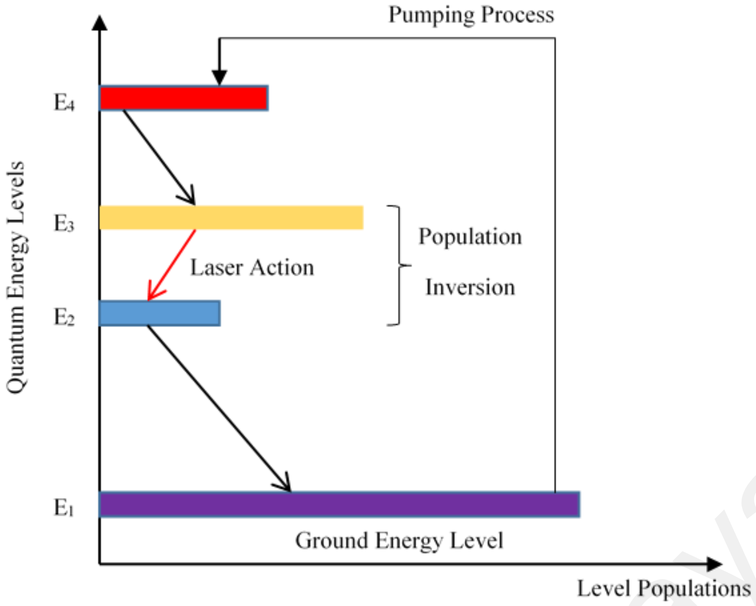

Figure 2.2: Energy diagram of a Four-level laser

The working principle of a four level laser pumping system is that electron is excited, or pumped (Chesler, Karr, & Geusic, 1970) from ground level to E_4 by means of collision with other atom of lasing medium or when high-energy radiation is absorbed. Let τ_{43}, τ_{32}, and τ_{21} be the time required for atoms to decay from 4 to 3, 3 to 2, and 2 to 1, respectively. In four-level system, $\tau_{21} >> \tau_{43} > \tau_{32}$, thus a population inversion would occur between E_3 and E_2 where photons flowing into the lasing medium will be amplified consistently.

Stimulated emission must be larger than absorption and spontaneous emission for a correct laser operation. High pumping rate is required for laser source with shorter wavelength. This is why maser was discovered first in 1953 by Charles H. Townes, H.J. Zeiger and James P. Gordon (Willner et al., 2012) (C. H. Townes, 1965) as the 24 GHz microwave had a relatively longer wavelength (~12.5 μm = 12500 nm) as compared to Maiman's pulsed red ruby (Cr^{3+}:Al_2O_3) laser that had the wavelength of ~695 nm, which is a visible light.

Emitted photons from the stimulated emission should not be allowed to escape. Optical resonator is a positive feedback mechanism that will allow continuous excitation of photons. Fundamental resonator consists of one highly reflective mirror and a partially reflective mirror. On-axis, desirable photons will be reflected back-and-forth by those mirrors, causing interactions with more atoms, which results in increase of stimulated emission and decrease of spontaneous emission. Small percentage of travelling photons will be coupled out of the system as usable laser through the partially reflective mirror. Setup for a basic laser is illustrated in Figure 2.3.

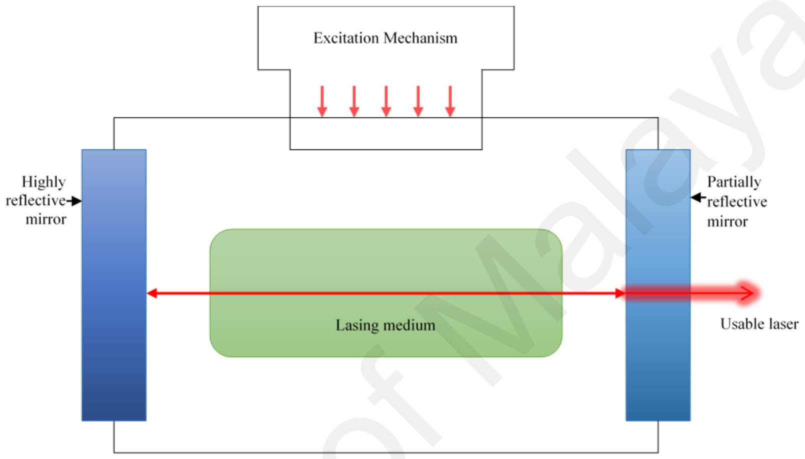

Figure 2.3: Basic laser setup

There are two major excitation or pumping methods, which are the optical pumping and electrical pumping. In optical pumping, an incoherent, continuous wave (cw) or pulsed light radiated by a powerful light or laser is absorbed by the lasing medium, causing population inversion. This method is applicable for dye lasers and solid-state lasers. In electrical pumping, intense electrical discharge of pulsed current or radio frequency (RF) wave flowed into active medium such as semiconductor or ionized gas (Harun, 2016). Other pumping methods are irradiation by electron pumping, X-Ray pumping, and chemical reaction pumping.

2.2.4 Types of Laser and Their Applications

There are many ways to categorize laser. One of it is by basing on the pumping level. Aside from four-level pumping system discussed earlier, there are also three-level system and quasi-three-level system. In three-level system, the laser action occurred when atoms returned to ground state from the metastable level 2. The first ruby laser by Maiman is an example of a three-level laser (Poprawe, Boucke, & Hoffman, 2018). Meanwhile, a quasi-three-level system is a unique case where there is a lower energy level that exists so close to the ground level. In thermal equilibrium, this lower level has a population. The operating principle of quasi-three-level laser is similar to a four-level laser, except there is a trade-off between efficient pump absorption and short wavelength operation. Example of lasers classified by pumping level are shown in Table 2.1.

Table 2.1: Laser classification by pumping level

Laser pumping	Example	Absorption Wavelength (nm)
Three-level	Ruby	694.3
Quasi-three-level	Nd:CNGG (Tan, Chen, Aldana, Yu, & Zhang, 2015)	890 - 930
Four-level	Nd:YAG	730 – 760 and 790 - 820

Next, lasers can also be categorized according to their duration of emission. In cw laser, light is emitted for a longer time, resulting an observable laser with low power. One such laser is YbAG that can be operated at room temperature (Kimura et al., 2013). Advantages of such laser are its small size, high stability and isotropic. For laser operating in pulsed mode, the beam is radiated over a short time (ns to ps) that produces high energy laser. Such laser is beneficial for drilling for sub-µm holes on printed circuit board (PCB), as demonstrated by work of (D. Lee, 2017).

Table 2.2: Laser classification by operating mode

Operation mode	**Example**	**Operating wavelength (nm)**
cw	YbAG	920
Pulsed	IR pulsed	1030

Moving forward, lasers taxonomy can also be done by studying the type of active material used. These active materials exist in one of these states; solid-state, dye (liquid), gas, excimer or semiconductor.

As its name implied, a solid-state laser is one that uses a solid active medium. Even though semiconductor is also a solid, it is regarded as a different active medium due to the later electrical conduction properties. One advantage of solid-state laser over semiconductor laser is that when a solid-state is doped with rare-earth elements such as Er or Yb that have longer upper state lifetimes compared to semiconductor, relative intensity noise (RIN) of the laser is lowered (Grubb, Leilabady, & Frymyer, 1993). RIN, or white noise, is an important parameter when measuring quality of a fiber used in communication. One source of RIN is spontaneous emission (Hashemi, 2012).

For dye or liquid active medium such as rhodamine 6G, when the medium is pumped with pulsed laser excitation, atoms that are population-inverted increase significantly (Hammond & Nelson, 1980), which in return, produces high output power. A recorded power of 1.4 kW was attained when rhodamine 6G was mixed with solution of COT

(Manna & Saha, 2011). Further research using colloidal solution of gold and platinum nanoparticles dissolved with rhodamine 6G showed the absorption wavelength of rhodamine 6G could be decreased to 530 nm (Donchenko, Zinoviev, Zemlyanov, Kharenkov, & Panamaryova, 2016).

Next, in gas laser, electric current is discharged inside gas active medium, causing population inversion that results in laser emission. Mid-IR laser structure made up of CO and CO_2 lasers with range of operating wavelength from 2500 nm to 16600 nm was developed by (Kotkov et al., 2016). Early researches on gas lasers were limited by the poisonous and corrosive nature of some gasses, but with relatively harmless nitrogen N_2 gas as active medium, lasers pulses with duration over 220 ns operating at wavelength of 337.1 nm was actualized by (Kekez, 2018).

Excimer is a portmanteau of the word "excited" and "dimer", with dimer referring to a molecule with two comparable atoms. An excimer active medium is a blend of noble gas such as xenon (Xe) and argon (Ar), with halogen gas, such as chlorine (Cl) and fluorine (F). Operating wavelength for excimer laser is very short, producing light in ultraviolet region of the EM spectrum (157 nm to 351nm) with high energy and narrow pulse width. Organic optical data storage could be imprinted to human hair using excimer laser, as the laser is precise in evaporating molecular bonds of human tissues without heat generation (Kanade, 2017). This laser technology is what enabling IoT.

Finally, semiconductor lasers work using the principle of moving holes and electron between valence band and conduction band of a semiconductor active medium. Photon with bandgap energy is emitted when electron recombined with holes. Vertical-cavity surface emitting laser (VCSEL) based on GaAs has been tested to produce 100 gigabits-per second (Gbps) data transmission (Deppe, Li, Yang, & Bayat, 2018).

Type of lasers using each category of active medium with its common operating wavelength and their regular applications are tabulated in Table 2.3 as investigated by (Jeff, 2008), (Ferrar, 1969), (Uchida, Agatsuma, Hashizu, Yamamoto, & Ikeda, 2006), (Valster et al., 1998) and (Krishna & Madhan, 2016).

Table 2.3: Lasers and their applications

Active Medium	Laser	Wavelength (nm)	Applications
Solid	Ruby	694.3	Dermatology, tattoo removal, holography
	Nd:YVO_4	1064	Green laser pointer
	Ho:YAG	2100	Kidney stone removal,
Dye	Rhodoamine 6G	450 - 650	Medicine, spectroscopy
	Coumarin	460 - 515	Insecticides
Gas	CO_2	9600 - 10600	Welding, cutting
	HeNe	632.8 nm	Barcode scanner
Excimer	ArF	193	LASIK eye surgery
	Krf	248	Lithography
Semiconductor	GaN	400	Optical Blu ray reading/recording
	AlGaAs	780	Laser printer
	VCSEL	850 - 1500	Gigabit fiber

2.2.5 Tunable Laser

Tunable laser is defined as a laser with adjustable output wavelength. As shown in Table 2.3 earlier, certain lasers have their own wavelength operating range, broad or narrow. In wavelength division multiplexing (WDM) fiber optics network that employ fixed-wavelength beam, tunable laser transmitter is important to reduce the cost of the networks by decreasing the inventory of laser transmitters including for speed upgrade purpose (Buus & Murphy, 2006).

There are generally three mechanisms of laser tuning: Birefringent filters, littrow prisms, and diffraction gratings. The coatings of the resonators or cavity must be adequately broadband to cater to the entire tuning range of the laser. Birefringent filters are used in continuously tunable Ti-Sapphire solid state and dye lasers (Dhirhe, Slight, Holmes, Hutchings, & Ironside, 2013). One generic design of a birefringent filter is illustrated in Figure 2.4.

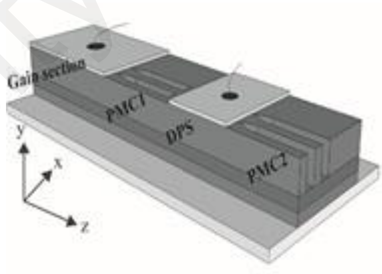

Figure 2.4: Generic design of a Birefringent filter

The filter above is made up of polarization mode convertors (PMCs) that convert transverse magnetic (TM) polarized light coming from the gain section into a circularly-polarized light. The differential phase shift (DPS) is a 2 quarter waveplates where the birefringence can be adjusted by injection current. The relative phase of circularly-polarized light from PMC 1 is tuned by the DPS. The polarization of the output laser is regulated at by PMC 2. The wavelength of the laser is tuned by line-narrowing effect of the DPS.

Since gas laser has a wide range of operating wavelength (from UV to near IR), littrow prism are used extensively as tuning mechanism. Simplest form of littrow prism is depicted in Figure 2.5 (Ilev, Waynant, Kumagai, & Midorikawa, 1999). Littrow prism is a 30/60 right triangle prism, with the surface opposite of the 60-degree angle is coated with a broadband high-reflective mirror coating. The prism is tuned or rotated to angles where desired wavelength is reflected back on-axis, while the non-desirable wavelengths are mirrored off-axis.

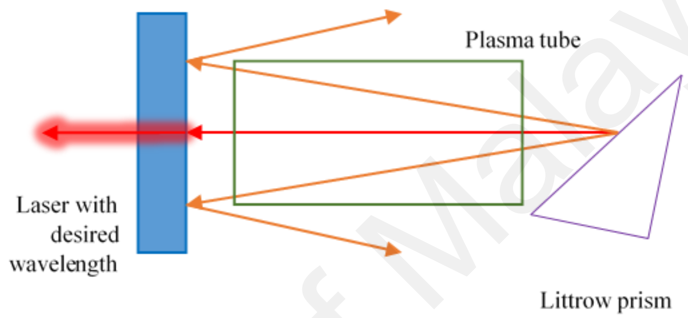

Figure 2.5: Basic mechanism for litrrow prism tuning

Mechanism of laser tuning by diffraction grating is similar to littrow prism, but it is used by laser systems that require higher degree of dispersion of unwanted wavelengths. Different peak powers are provided at different grating orders (Alhazime et al., 2013), (Cataluna, Ding, Nikitichev, Fedorova, & Rafailov, 2011).

2.3 Q-Switching

Unlike mode-locking which produces pulsed laser with short duration (narrow pulse) as small as pico- to femto-seconds, Q-switching yields pulsed laser with duration in the vicinity of nano- to micro-seconds. Peak power generated by Q-switching methods ranges from μW to GW, which is smaller than mode-locking method, owning to the broader pulse width. One important parameter in Q-switching is the unit-less quality Q factor of the optical resonator discussed earlier in subchapter 2.1. It is defined as the ratio of resonance frequency, υ_0, to the full width at half-maximum (FWHM), $\delta\upsilon$, of the resonance.

$$Q = \frac{\upsilon}{\delta\upsilon} \qquad (2.7)$$

2.3.1 Active Q-Switch

Mechanical switches such as rotating mirrors placed at ends of laser resonators are employed in active Q-switching. Modulators such as electro-optic (EOM) that tune the polarization or phase of a laser beam, or acousto-optic (AOM) that set the frequency or spatial direction of a laser, could also be used in the same switching method. These extra components would increase the cost to build a laser. Power produced through active Q-switched is very high, with Fiber Bragg grating Q-switched was reported to produce peak power of 5.6 W with pulse width of 450 ns (Monga, Meyer, & Manuel, 2017). Although more physical space is required in an active Q-switch setup than the passive one, it is still doable in a lab.

General overview of the gains and losses of an active Q-switched laser against time is illustrated in Figure 2.6. Arbitrary unit (a.u.) of output power is assigned to the y-axis on the oscilloscope trace as output power can be in the range of microwatts to milliwatts. After the active Q-switched is turned on at time t = 0, the output power started to climb in exponential manner and become extremely high after 0.2 µs. Switching time is not necessary to be equal of the pulse width, as the formation of pulse required numerous resonators round trips.

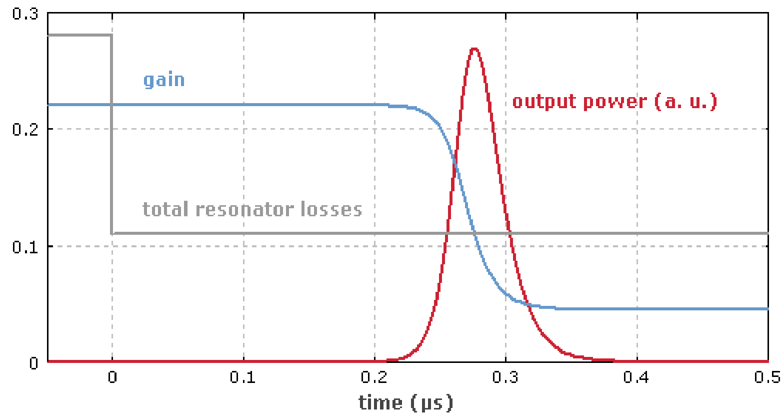

Figure 2.6: Gain and Losses vs Time in Active Q-switching

2.3.2 Passive Q-Switch

Benefits of passive Q-switch such as low cost, flexible design, compactness, and minimalism have encouraged researches throughout the years. The rose gold-based SA used in this dissertation has a cross-section of 1 mm x 1 mm. SA such as Transition-metal dichalcogenide (TMD) has been found to output peak power of 8.7 mW with pulse duration as fast as 200 ns (D. Wu et al., 2017). SA synthesized from layers of black phosphorus was able to attain peak power of 13.12 mW at 1550 ns pulse width while producing laser operating at wavelength of 1029.63 nm (J. Wang et al., 2018). Similarly, the gain and losses of a passive Q-switch over time is generalized in Figure 2.7.

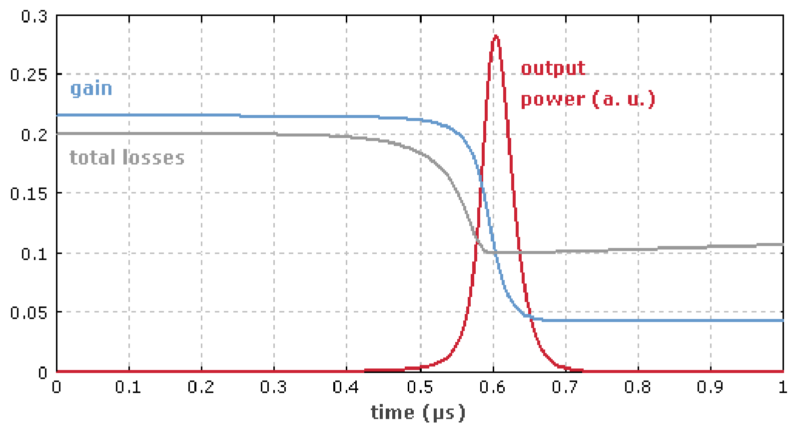

Figure 2.7: Gain and Losses vs Time in Passive Q-switching

2.4 Saturable Absorber

Small in size, SA is a nonlinear optical material with optical loss that is inversely proportional to the incident laser intensity. Lasers of different types (solid-state, doped-fiber, or semiconductor) make use of SA due to its desired properties such as broadband absorption, low saturation intensity, high modulation depth, and ultrafast recovery time ranging from ps to ns. SA such as Zirconium Boride (ZrB_{12}) is researched due to its very high melting points of above 3000 °C, which makes it suitable for aerospace applications (Hattori, Haque, Olbricht, & Li, 2018). There are two types of SA, namely artificial SA and real SA. Artificial SAs are materials that do not absorb light but still produce optical losses, such as Kerr lens (L. Wang, Chong, & Haus, 2016) and loop-mirror-filter (LMF) (Havstad, Fischer, Willner, & Wickham, 1999). Only real SAs that absorb light are considered when writing this dissertation.

There are three mains traits that are required for a good SA. The SA must have a longer recovery time for the absorber as compared to the pulse duration, but ample enough to ensure the optical loss is recovered prior to gain after laser pulse emission. Next, the saturation energy of a SA must be higher than the saturation gains of the active medium so that the saturation of the SA is fast and loss in pulse energy is reduced. Lastly, for peak pulse energy, the modulation depth (maximum loss reduction) should be in the region of one and half (1.5) times of the initial gain and non-saturable losses must be as minimum as possible. Smaller modulation depth is preferable in case of low pulse energy with high repetition rate.

Working principle of SA is exemplified in Figure 2.8. Let $h\upsilon$ be the energy of incident photon, E_V is energy at valence band, E_C is energy at conduction band, and $E_G = E_V – E_C$ is the SA bandgap energy. When a photon impinges on the SA, light will absorbed by the SA if $h\upsilon$ is higher than E_G, to excite carriers from having E_V to E_C. Electron-hole carrier pairs are generated through this process. Conforming to Pauli Exclusion Principle, SA would be in saturated mode when there are no more photons that could be absorbed due to conduction band is fully occupied with excited carriers. SA is transparent then.

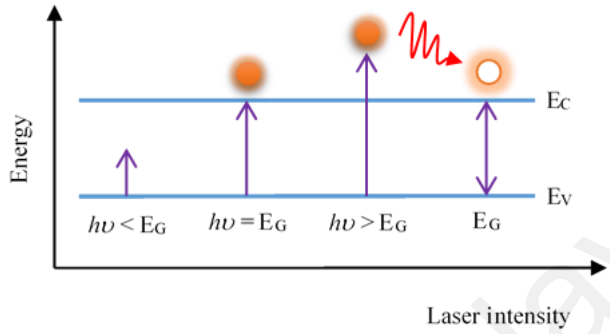

Figure 2.8: Process of saturable absorption

During SA saturated state, electron-hole recombination and absorption of excited state are stimulated by additional photons that pass through the SA. Substantial photons released are induced by this effect, where abrupt intense light is generated, and carrier pairs would drop back to the ground (valence) state. This is followed by the reducing laser intensity and saturable absorption of the SA would recover, and the process is repeated. The described process is illustrated in Figure 2.9.

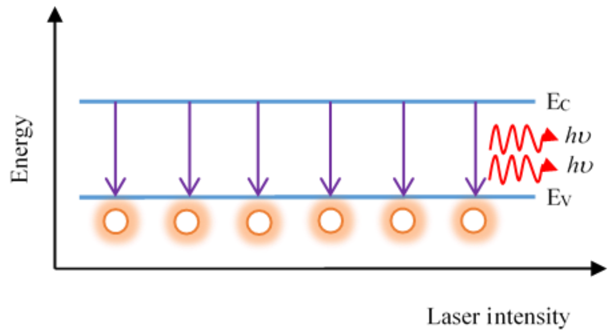

Figure 2.9: Photons emitted by saturated SA

2.5 Gold

In this dissertation, gold in the color of rose was utilized as a SA. Gold is a transition element or transition metal with atomic number 79. It is pronounced as *Aurum* in Chemistry (Au in the periodic element), a Latin word relating to Aurora, Roman goddess of dawn (Gimeno, 2008).

There are three salient characteristics of gold. Firstly, the ductility, which means the ability to be stretched, and malleability, which is the ability to be compressed, of gold are large. Gold in a quantity of 28.3 grams (1 ounce) could be flatten out up to 1 square meter (m^2). Next, gold does not rust (oxidized) in atmosphere at room temperature. It also does not react chemically to most acids and alkalis. Lastly, the yellow color of the gold is the effect of blue and green photons being absorbed by valence electron of gold.

As shown in Table 2.4 (Kopeliovich, 2014), rose gold is a composition of gold, silver (Ag) and copper (Cu). Different ratio of mixture of those three elements would produce different color. Pink gold and red gold are also considered to be rose gold.

Table 2.4: Gold alloys

Carat purity and color	Au,%	Ag,%	Cu,%	Pd,%	Pt,%	Ni,%	Zn,%	Fe,%	Cd,%	Al,%
24K Yellow Gold	99.7 min.	-	-	-	-	-	-	-	-	-
22K Yellow Gold	92	4	4	-	-	-	-	-	-	-
22K Yellow Gold	91.7	5	2	-	-	-	1.3	-	-	-
18K Yellow Gold	75	15	10	-	-	-	-	-	-	-
18K Red Gold	75	-	25	-	-	-	-	-	-	-
18K Rose Gold	75	2.75	22.25	-	-	-	-	-	-	-
18K Pink Gold	75	5	20	-	-	-	-	-	-	-
18K White Gold	75	-	-	25	-	-	-	-	-	-
18K White Gold	75	-	-	-	25	-	-	-	-	-
70Gold-30Pt	75	-	-	-	30	-	-	-	-	-
18K White Gold	75	-	-	10	-	10	5	-	-	-
18K White Gold	75	18.5	1	-	-	-	5.5	-	-	-
18K Blue Gold	75	-	-	-	-	-	-	25	-	-
18K Grey-White Gold	75	-	8	-	-	-	-	17	-	-
18K Green Gold	75	20	5	-	-	-	-	-	-	-
18K Light Green Gold	75	-	23	-	-	-	-	-	2	-
18K Soft Green Gold	75	25	-	-	-	-	-	-	-	-
18K Deep Green Gold	75	15	6	-	-	-	-	-	4	-
18K Purple Gold	80	-	-	-	-	-	-	-	-	20
14K Yellow Gold	58	28-Apr	14-28	-	-	-	-	-	-	-
14K White Gold	59	-	25.5	-	-	12.3	3.2	-	-	-
14K Green Gold	58.3	32.5	9	-	-	-	0.2	-	-	-
9K Yellow Gold	37.5	12.1	44.4	-	-	-	6	-	-	-
9K White Gold	37.5	-	34	-	-	17.7	10.8	-	-	-

As a SA, owning to its large third order nonlinearity, large electromagnetic-field enhancement, and fast recovery time, concave gold bipyramids SA has recorded an average output power of 9.61 mW with pulse width of 1.83 µs (H. Wu et al., 2018). It is a promising prospect for a pulsed laser.

2.6 Optical Parameters

Throughout this report, several optical parameters have been mentioned. They are revisited in this section to be given clearer definition.

2.6.1 Repetition Rate, R_r

R_r is defined as number of pulses emanated per second. The parameter R_r is inversely proportional to the pulse width, and co-varied with changes in pump power of the laser. It is measured by oscilloscope.

2.6.2 Pulse Width or Pulse Duration, Δt

Pulse width is demarcated as the width (duration) of the pulse at half peak power. The shape of the pulse is characterized using Gaussian function.

2.6.3 Pulse Energy, E_p

E_p is the sum of optical energy contained in a pulse. It is computed by dividing the average output power, P_{out} (obtained by optical power meter), by the repetition rate, R_r.

$$E_P = \frac{P_{out}}{R_r} \qquad (2.8)$$

2.6.4 Peak Power, P_p

Peak power, P_p, is the maximum output power of a pulse. It is computed using the equation:

$$P_p = f_s \frac{E_P}{\Delta t} \qquad (2.9)$$

where f_s is a numerical factor affected by the pulse shape. Pulse that has the shape of sech^2-function has f_s value of 0.88 while Gausian pulse has a f_s value of 0.94.

2.6.5 Laser Efficiency, η

Also known as differential efficiency or slope efficiency, η is defined as the slope of a curve obtained by plotting the output power of the laser, P_{out}, against the pump power, P_{pump}.

$$\eta = \frac{P_{out}}{P_{pump}} \qquad (2.10)$$

The above parameters are illustrated in Figure 2.10.

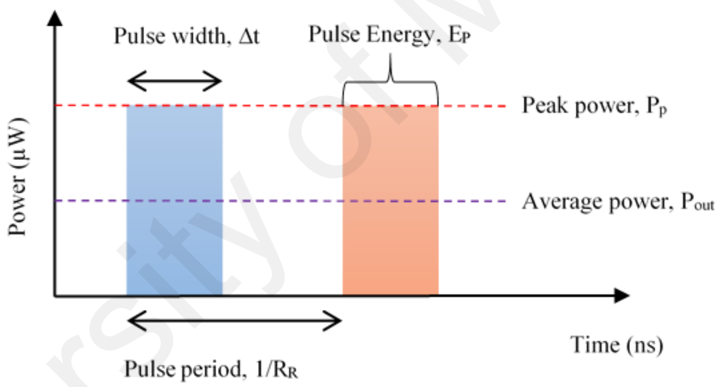

Figure 2.10: Optical parameters

CHAPTER 3: METHODOLOGY

3.1 Introduction

Laser with a pulse train that has high energy, high repetition rate, and low pulse width is preferred for various application. One method to produce such pulse is by using SA in Q-switching technique. In this chapter, the process of fabricating rose gold-based SA and how the experiment is set up are outlined concisely.

3.2 Fabrication and Characterization of Rose Gold-based SA

Gold (III) chloride trihydrate ($HAuCl_4$) (~50% Au-based) and Polysodium-4-styrenesulfonate (PSSS) were procured from Sigma-Aldrich Corporation, Wisconsin, America, and at the same time sodium borohydrate ($NaBH_4$) and tri–sodium citrate, TSC ($Na_3C_6H_5O_7$) were bought from R&M Marketing, United Kingdom. All solutions were prepared using deionized water that had a resistivity of 18.0 MΩ. No further purifications were performed on all solvents and chemicals as they were utilized as they were received. Handling of the materials and chemicals synthetization were conducted in a fume closet.

$NaBH_4$ reduction method was employed to prepare the Au nanoparticles (NPs). The Au NPs were readied initially with the mixing of 3 mL of $NaBH_4$, 3 mL of PSSS, and 50 mL of TSC, into a beaker containing 1000 mL of deionized water. The solution was then stirred at 450 RPM. 50 mL of $HAuCl_4$ (5 mm in water) were added dropwise at the rate of 2 mL/min into the mixture with continuous stirring. This is proceeded with the addition of the excess amount of 20 mL of TSC. The reaction was allowed for 5 minutes at room temperature before finally centrifugation was performed for cleaning purpose. The resultant Au NPs were used for synthetization of thin films of SA that have a surface area of 1 mm^2 (1mm x 1mm) per-film in color of rose gold. The finalized SA is illustrated in Figure 3.1.

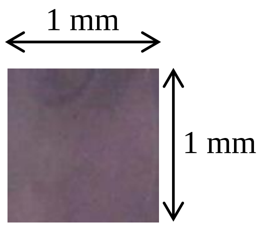

Figure 3.1: 1 mm^2 rose gold-based SA

UV–vis spectroscopy by Shimadzu was used to characterize the aqueous products in scale of 300 nm to 1000 nm wavelength. The sizes of the NPs were quantified by using transmission electron microscopy (TEM) imaging together with the identification of NPs morphology. Rigaku miniflex X-ray diffraction (XRD) with Cu K-alpha and Ni radiation filters at 0.02 degree per minute was utilized for X-ray dispersive analysis to further verify the lattice and morphology dimensions of AU NPs. Field emission scanning electron microscopy (FESEM) image of the resultant AU NPs was depicted in Figure 3.1. AU NPs that have nano-plate with the edge size ranging from 50 nm to 150 nm were observed (Morsin, Salleh, & Umar, 2014). The shapes of the NPs also varied from symmetric and asymmetric hexagonal, to spherical and irregular.

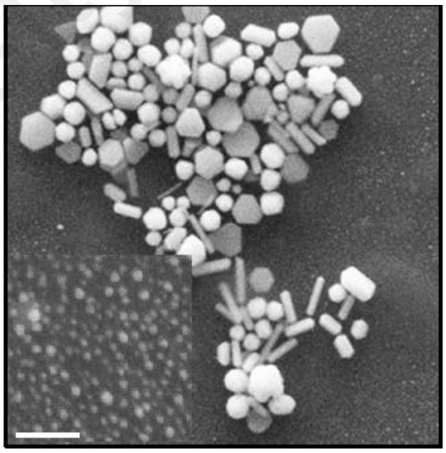

Figure 3.2: FESEM image of gold NPs

From XRD spectrum, it was discerned that the AU NPs have dual sharp peaks at 39.145° (marked as 111 in Intensity) and 44.3° (200), and the FWHM was 0.307. The XRD analysis outcome of the rose AU NPs was rendered in Figure 3.3.

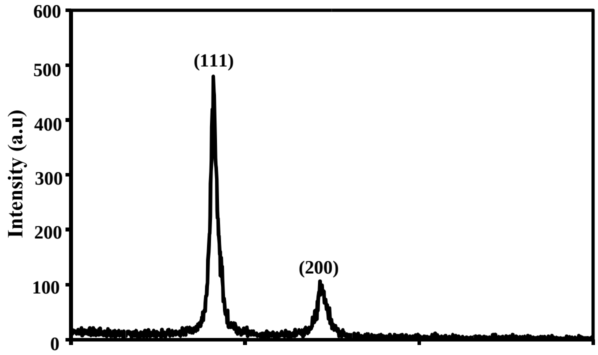

Figure 3.3: XRD results of Au NPs

3.3 Laser Cavity Configuration

The fabricated rose gold-based SA was slotted in between two fiber connectors (FCs) through a fiber adapter to create a fiber-compatible SA as shown in Figure 3.4. Optical gel is applied on the SA to ensure proper joining between the FCs. It was then incorporated into the laser cavity for the Q-switching procedure.

Figure 3.4: Positioning the SA between FC

A 3 m long Erbium-doped fiber (EDF) was exploited as a gain medium. The EDF was pumped with a 980 nm single-mode (SM) laser diode (LD), coupled through a 980/1550-nm fused wavelength division multiplexer (WDM). The EDF has the following specifications: manufactured by Fibercore; core diameter of 4 µm and cladding diameter of 125 µm; numerical aperture (NA) of 0.16; Iso-Gain I-25(980/125); cut-off wavelength in the range of 900–970 nm; and Erbium ion absorption rate of 23 dB/m at 980 nm. An isolator was used after the WDM to prevent reflection inside the ring cavity and to ensure unidirectional light propagation. FCs containing the SA were placed after the isolator. An 80/20 fiber coupler was assigned into the cavity after the FCs. The fiber coupler allowed 80% of the light to travel within the ring cavity while the 20% output was extracted towards equipment for analysis. Standard single mode fiber (SMF-28) was utilized for the remaining of the fibers.

A number of equipment were used for measurement of related optical parameters. A 500 MHz Yokogawa DLM2054 oscilloscope (OSC) connected with a 1.2-GHz photo-detector was used to monitor the laser spectrum, while an Anritsu MS2683A RF-spectrum analyzer was deployed to monitor the RF spectrum. An optical power meter was utilized to gauge the output power. Finally, a YOKOGAWA AQ6370C optical spectrum analyzer (OSA) was used to observe the time profile of the output pulse train. Measurements were taken in step of 10 mW for input pump power, from the minimum to maximum pump power threshold. The experimental setup for testing rose-gold based SA is illustrated in Figure 3.5.

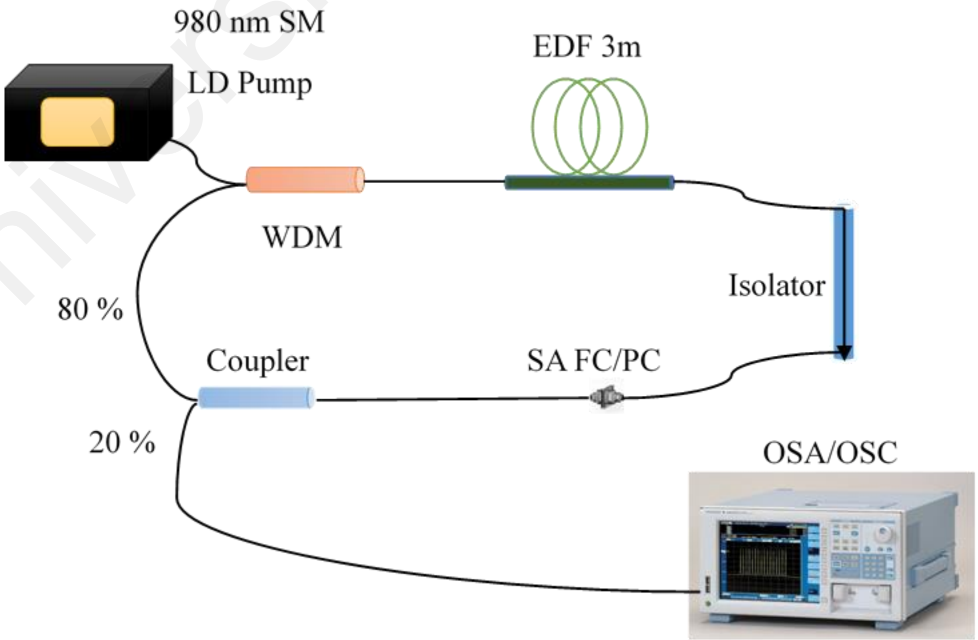

Figure 3.5: Laser ring cavity diagram for rose gold-based SA experiment

Before the experiment was started, the stability of the pulse laser at every tuned output wavelength was ensured by obtaining stable recording of output voltage using the oscilloscope. Oscilloscope traces at minimum and maximum threshold of the input pump power for tuned 1550.17 nm laser are shown in Figure 3.6.

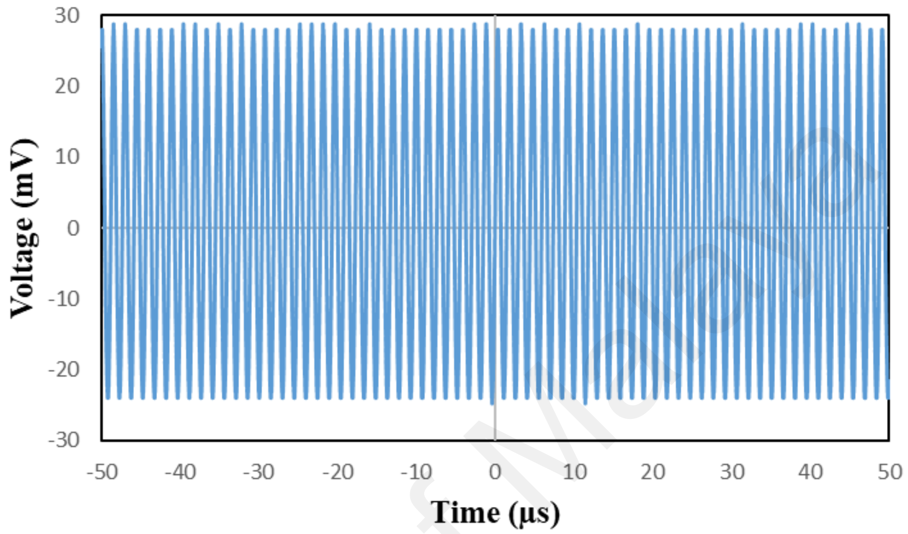

(a)

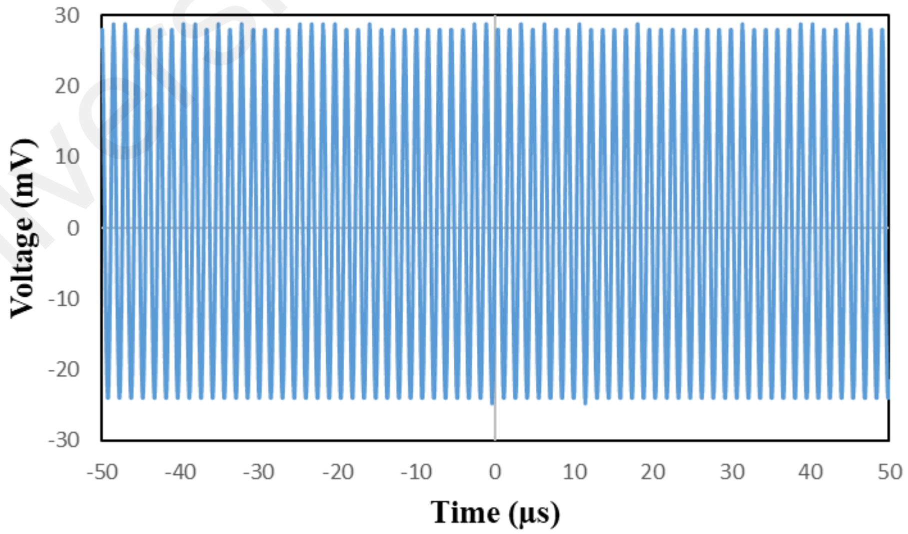

(b)

Figure 3.6: Oscilloscope traces of 1550.17 nm tuned laser with pump power (a) minimum 45 mW and (b) maximum 165 mW

CHAPTER 4: RESULTS AND DISCUSSION

4.1 Introduction

Self-made SAs are continuously researched in order to fabricate a SA that would have wide saturable absorption band, ultrafast response, and large third order nonlinear effects, such as absorption and refraction. The optical parameters obtained by using rose gold-based SA as a Q-switch for tunable laser is discussed in this chapter.

4.2 Tunable Q-switched Laser Using Rose Gold-based SA

The outputs of the laser cavity were tuned to produce three peaks of operating wavelengths at 1539.88 nm, 1550.17 nm, and 1560.21 nm. The lasers peak output powers were -13.675 dBm, -11.246 dBm, and -8.704 dBm, respectively, when the cavity was pumped by lowest threshold of the SA input power. The 3-dB bandwidth for each laser output were 0.035 nm, 0.05 nm, and 0.05 nm, in previously given order. Output spectrum of the working laser is shown in Figure 4.1.

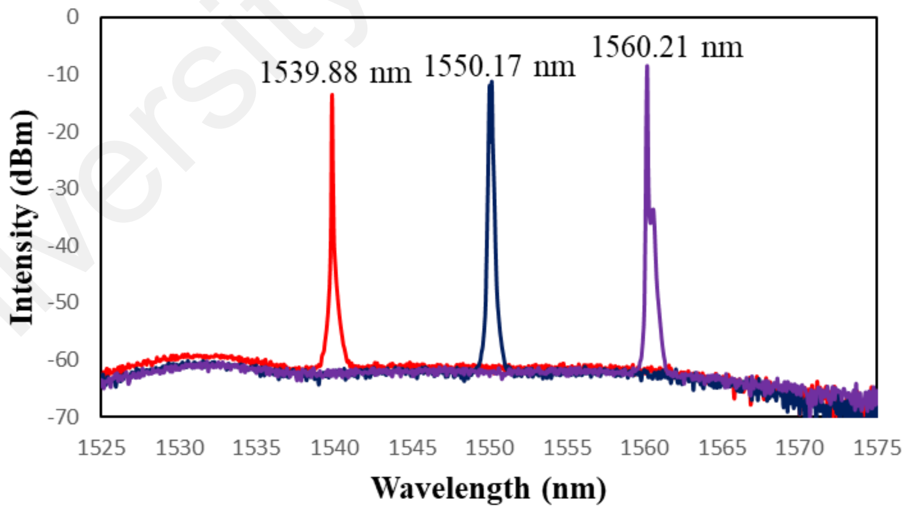

Figure 4.1: Laser output wavelengths of tunable Q-switched laser using rose gold-based SA at minimum pump power

The lower and upper thresholds for input pump power for the three lasers were: 35 mW and 115 mW for 1539.88 nm laser; 45 mW and 165 mW for 1550.17 nm laser; and

40 mW and 170 mW for 1560.21 nm laser. Beyond the ranges, rose gold-based SA would fail to act as a Q-switch for the tunable laser. In each laser, their pulse width decreased steeply in the initial stage as input power pump was increased in the step of 10 mW. They then continued to decrease linearly as input pump power was increased. The ranges of the pulse width were 22.5 to 8.2 µs (1539.88 nm), 18.5 to 7 µs (1550.17nm), and 21.9 to 8.558 µs (1560.21 nm). The ranges of the emitted pulses per second for each laser were 21.98 to 59.17 kHz (1539.88 nm), 25.58 to 67.96 kHz (1550.17nm), and 21.83 to 57.22 kHz (1560.21 nm). Saturation rate of the rose gold-based SA was hastened by the power circulating in the laser ring-cavity as input pump power increased. The obtained parameters were shown in Figure 4.2. These outcomes obeyed what are to be expected from a passive Q-switching technique.

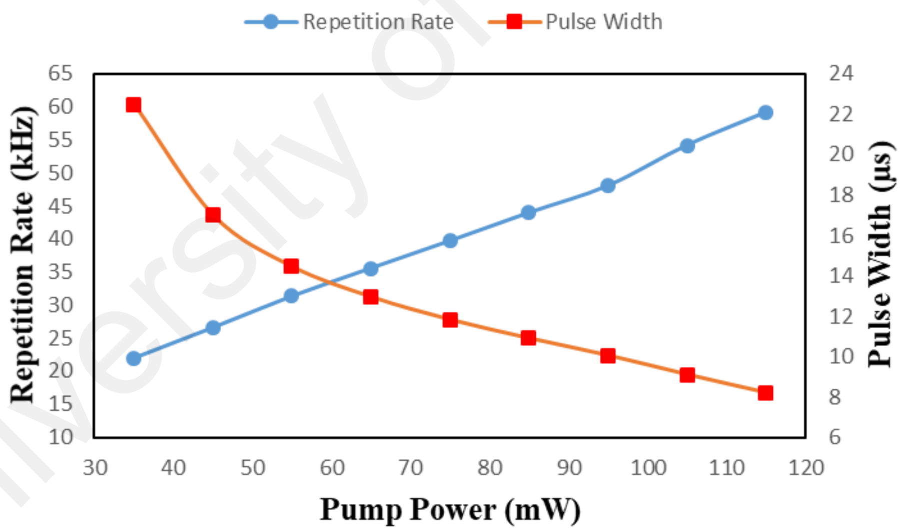

(a)

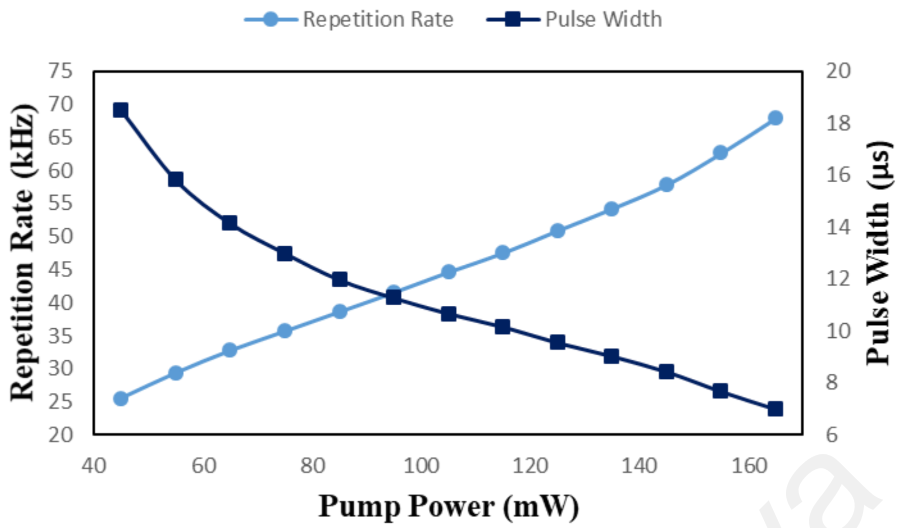

(b)

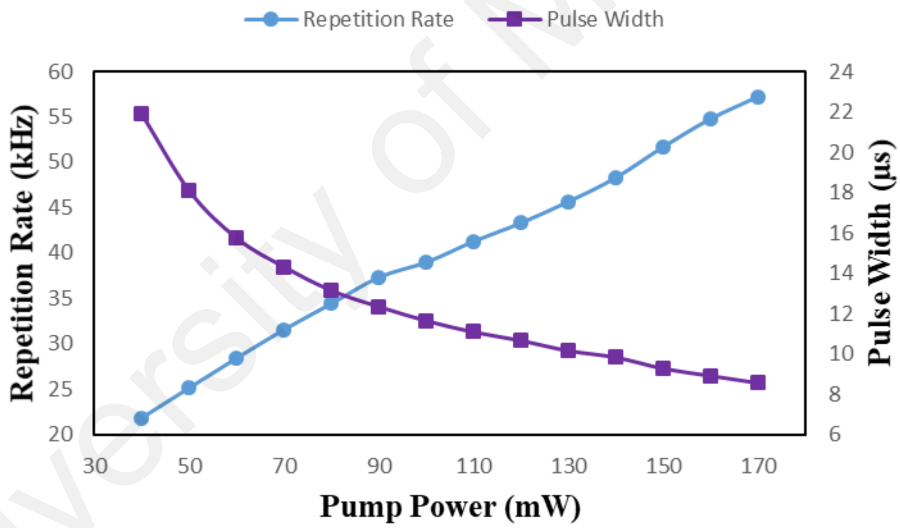

(c)

Figure 4.2: Repetition rate and pulse width of tuned-laser at (a) 1539.88 nm (b) 1550.17 nm (c) 1560.21 nm

The C-Band lasers had a maximum 19.77 nJ pulse energy and 1.17 mW output power for 1539.88 nm; 38.85 nJ and 2.64 mW for 1550.17 nm; and 41.24 nJ and 2.36 mW for 1560.21nm, when the input power pump was increased from their respective minimum to maximum threshold power. Accordingly, the laser efficiencies obtained were 1.296 %, 1.900 %, and 1.612 %. These results were reflected in Figure 4.3.

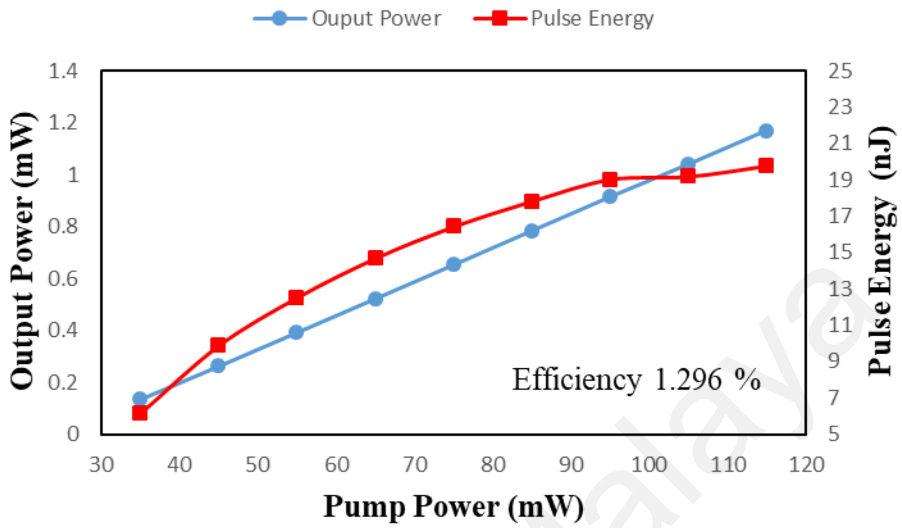

(a)

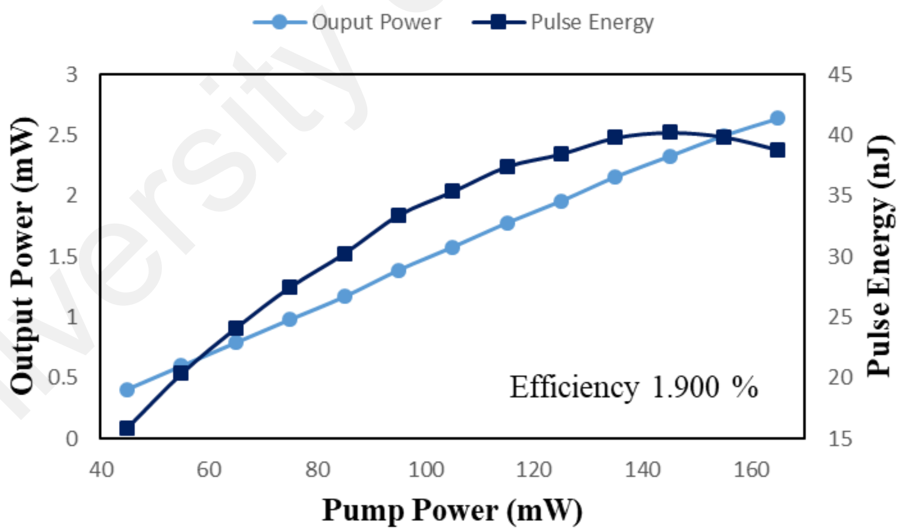

(b)

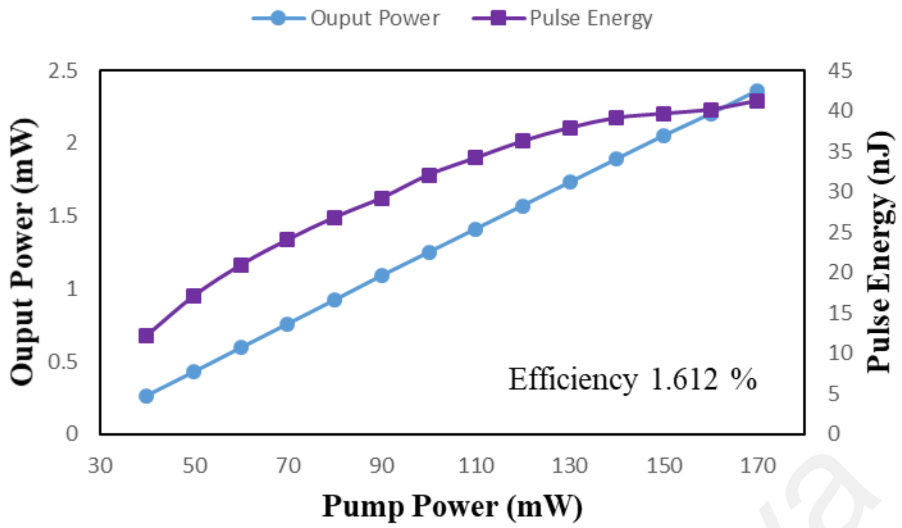

(c)

Figure 4.3: Output power and pulse energy at (a) 1539.88 nm (b) 1550.17 nm (c) 1560.21 nm

Single fundamental frequency was observed in the RF domain for each laser, thus validating the stability of the generated Q-switched pulses. No fluctuations were detected after the input pump power was increased beyond the threshold power. Signal-to-noise ratios (SNRs) of 48.52 dB (1539.88 nm) and 31.17 dB (1550.17 nm) and 43.77 dB (1560.21 nm) were obtained at maximum pump power for each lasers. They were illustrated in Figure 4.4.

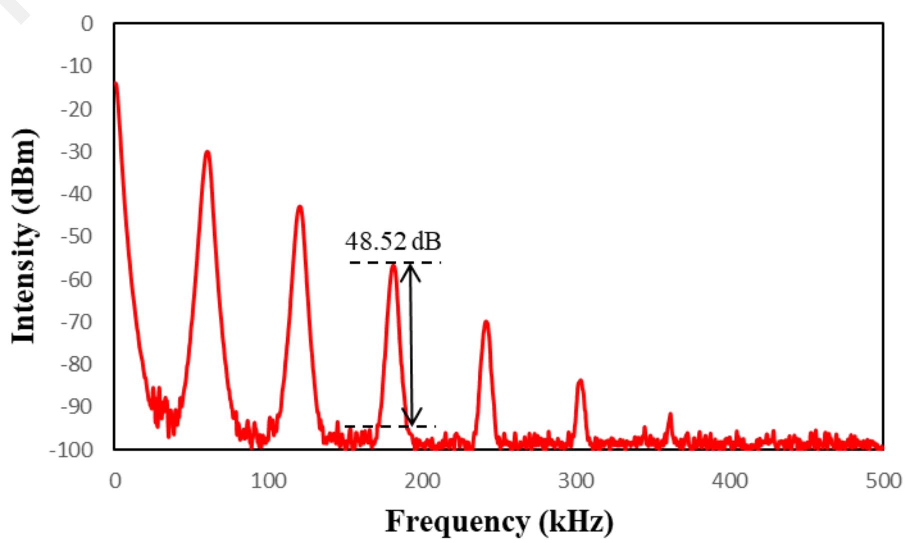

(a)

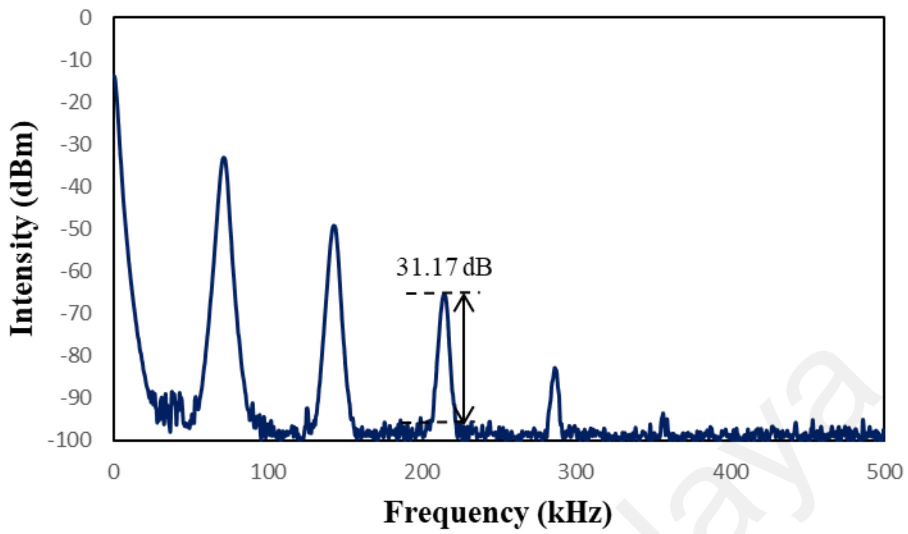

(b)

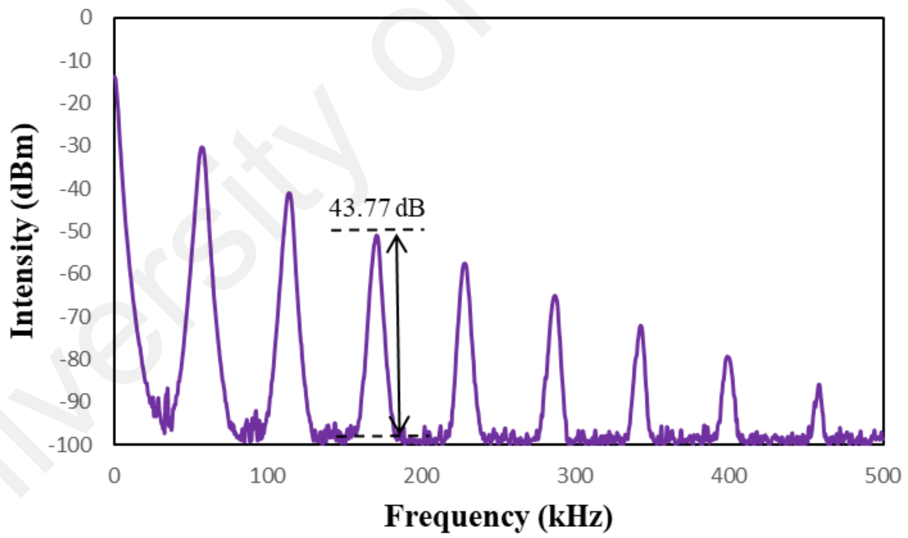

(c)

Figure 4.4: RF spectrum characteristics at maximum pump power (a) 1539.88 nm (b) 1550.17 nm (c) 1560.21 nm

4.3 Summary

From the results obtained, it was determined that the rose gold-based SA worked best for laser which output is tuned to wavelength of 1550.17 nm (193.5 GHz). Beyond 1565 nm region, the output powers were affected by background noises originated from the ambient temperature due to the transition between light and heat at IR wavelength.

The efficiency of 1.900 % is lower when compared to 6.9 % obtained by SA made from a mixture of gold nanorods (GNRs) and sodium carboxymetyl cellulose (NaCMC). However, the efficiency of rose gold-based SA was still higher than another self-produced gold-based SA done previously that had a 1.5% efficiency (J. Lee, Koo, Lee, & Lee, 2016). The efficiency obtained was also greater than polyvinyl alcohol (PVA)/graphene based SA with efficiency of 0.011% (Ahmad, Aidit, Thambiratnam, & Tiu, 2017) which was also synthesized in the same lab where the rose gold based-SA was produced.

The maximum recorded output power was found at laser tuned to 1550.17 nm output when 2.64 mW was yielded by 165 mW input power pump. This also proved that the ring cavity has low absorption rate at 1550 region, as what EDF should be.

SNR was traded with efficiency and output power as 1550.17 nm laser had wide range of input pump power that the SA could handle. The efficiency was attributed to low attenuation of the fiber ring cavity at 1550 nm region. The proposed SA is suitable for pairing with EDF laser operating at 1550 nm where loss of 0.2 dB/km is an advantage to reduce the overall cost of optical fiber networks.

CHAPTER 5: CONCLUSION

The first objective of this dissertation was accomplished when $HAuCl_4$ (gold solution) was mixed with the solution of PSSS, TSC and $NaBH_4$. This fabrication process is referred as $NaBH_4$ reduction method. The resultant Au NPs were cut and shaped into thin films to be used as the SA. The advantages of the reduction method are that it is rapid and simple. It also generated high yield where spares of rose gold-based SA thin films are stored for future use in other researches.

Next, the tunability of the laser was demonstrated when stable train of pulses were generated for three different output wavelengths. Rose gold-based SA has wide operating range for the input pump, which was from 45 mW to 165 mW for 1550.17 nm laser. Produced output power ranged from 406.05 μW to 2.64 mW. It was concluded that the SA fabricated worked well when paired with EDF laser.

The final objective was attained when the proposed SA was compared to previous works from various authors. The efficiency was higher than other self-made, passive SAs, but it was a lot lower than other gold-based SAs that were fabricated carefully.

Several methods are available to improve the obtained result. The lengths of EDF gain medium could be further extended to broaden the spectral wavelength. The output power is directly proportional to the length of the EDF (Al-Mashhadani et al., 2013) until a saturation point is arrived. Another solution to heighten the output power is by further reducing the reflectivity of the cavity. Methods recommended are external of the SA.

Future researches should focus on investigating the behavior of the SA in broader ranges of output laser wavelength, such as from 1300 nm to 1900 nm. Chemistry must be revisited intensively in order to further understand the properties of gold-based SAs and the optimum method to manufacture them.

REFERENCES

Ahmad, H., Aidit, S. N., Thambiratnam, K., & Tiu, Z. C. (2017). Passively Q-switched O-band praseodymium doped fluoride fibre laser with PVA/graphene based SA. *Electronics Letters*, *53*(22), 1481-1483. doi:10.1049/el.2017.2064

Al-Mashhadani, T. F., Jamaludin, M. Z., Al-Mansoori, M. H., Abdullah, F., Abass, A. K., & Ali, M. H. (2013, 28-30 Oct. 2013). *Impact of passive EDF length on the performance of linear cavity BEFL.* Paper presented at the 2013 IEEE 4th International Conference on Photonics (ICP).

Alhazime, A., Ding, Y., Nikitichev, D. I., Fedorova, K. A., Krestnikov, I. L., Krakowski, M., & Rafailov, E. U. (2013). Broadly tunable quantum-dot based ultra-short pulse laser system with different diffraction grating orders. *Electronics Letters, 49*(5), 364-366. doi:10.1049/el.2012.3761

Buus, J., & Murphy, E. J. (2006). Tunable lasers in optical networks. *Journal of Lightwave Technology, 24*(1), 5-11. doi:10.1109/JLT.2005.859839

Cataluna, M. A., Ding, Y., Nikitichev, D. I., Fedorova, K. A., & Rafailov, E. U. (2011). High-Power Versatile Picosecond Pulse Generation from Mode-Locked Quantum-Dot Laser Diodes. *IEEE Journal of Selected Topics in Quantum Electronics, 17*(5), 1302-1310. doi:10.1109/JSTQE.2011.2141119

Chesler, R. B., Karr, M. A., & Geusic, J. E. (1970). An experimental and theoretical study of high repetition rate Q-switched Nd: YA1G lasers. *Proceedings of the IEEE, 58*(12), 1899-1914. doi:10.1109/PROC.1970.8062

Davis, R. (2018). The last measurement of the speed of light [Basicmetrology]. *IEEE Instrumentation & Measurement Magazine, 21*(2), 26-28. doi:10.1109/MIM.2018.8327975

Deppe, D. G., Li, M., Yang, X., & Bayat, M. (2018). Advanced VCSEL Technology: Self-Heating and Intrinsic Modulation Response. *IEEE Journal of Quantum Electronics*, 1-1. doi:10.1109/JQE.2018.2826718

Dhirhe, D., Slight, T. J., Holmes, B. M., Hutchings, D. C., & Ironside, C. N. (2013, 12-16 May 2013). *Wavelength tuning and polarisation control with an integrated tunable birefringent filter for quantum cascade lasers.* Paper presented at the 2013 Conference on Lasers & Electro-Optics Europe & International Quantum Electronics Conference CLEO EUROPE/IQEC.

Donchenko, V. A., Zinoviev, M. M., Zemlyanov, A. A., Kharenkov, V. A., & Panamaryova, A. N. (2016, June 30 2016-July 4 2016). *The laser generation threshold characteristics of a colloidal solution of gold and platinum nanoparticles with rodamine 6G.* Paper presented at the 2016 17th International Conference of Young Specialists on Micro/Nanotechnologies and Electron Devices (EDM).

Ferrar, C. (1969). Mode-locked flashlamp-pumped coumarin dye laser at 4600 &#197. *IEEE Journal of Quantum Electronics, 5*(11), 550-551. doi:10.1109/JQE.1969.1075697

Foth, H.-J. (2008). Principle of Lasers. In M. Lacner (Ed.), *Lasers in Chemistry Vol 1: Probing Matter* (pp. 30). Weinheim, Germany: Wiley.

Gene, J., Kim, S. K., & Lim, S. D. (2018). Validity Analysis of Holmium-Doped Fiber as Saturable Absorber for Passively Q-Switched Thulium-Doped Fiber Laser. *Journal of Lightwave Technology, 36*(11), 2183-2187. doi:10.1109/JLT.2018.2806963

Gimeno, M. C. (2008). The Chemistry of Gold. In A. Laguna (Ed.), *Modern Supramolecular Gold Chemistry: Gold-Metal Interactions and Applications* (pp. 64). Weinheim German: WILEY.

Grubb, S. G., Leilabady, P. A., & Frymyer, D. E. (1993). Solid-state laser pumping of 1.5 um optical amplifiers and sources for lightwave video transmission. *Journal of Lightwave Technology, 11*(1), 27-33. doi:10.1109/50.210567

Hammond, P., & Nelson, R. (1980). Radiation trapping in a laser dye medium, rhodamine 6G in alcohol. *IEEE Journal of Quantum Electronics*, *16*(11), 1161-1163. doi:10.1109/JQE.1980.1070402

Harun, S. W. (Producer). (2016, 2016). Laser Lecture 3b. Retrieved from https://casv.um.edu.my/cas/loginAllType?service=http%3A%2F%2Fspectrum.um.edu.my%2Flogin%2Findex.php

Hashemi, S. E. (2012). *Relative Intensity Noise (RIN) in High Speed VCSELS for Short Reach Communication.* (Master of Science Thesis in Photonics Engineering), Chalmers University of Technology, Goteborg, Sweden.

Hattori, H. T., Haque, A., Olbricht, B. C., & Li, Z. (2018). Zirconium Boride as a High Fluence Saturable Absorber for Q-Switched Fiber Lasers. *IEEE Photonics Technology Letters, 30*(1), 11-14. doi:10.1109/LPT.2017.2771224

Havstad, S. A., Fischer, B., Willner, A. E., & Wickham, M. G. (1999, 21-26 Feb. 1999). *Dynamic fiber loop-mirror-filter (LMF) based on pump-induced saturable gain or absorber gratings.* Paper presented at the OFC/IOOC . Technical Digest. Optical Fiber Communication Conference, 1999, and the International Conference on Integrated Optics and Optical Fiber Communication.

Hitz, C. B., Ewing, J. J., & hect, J. (2012). *Introduction to Laser Technology, 4th Edition*. Piscataway, NJ: John Wiley & Sons.

Huang, K. Y., Su, C. K., Lin, M. W., Chiu, Y. C., & Huang, Y. C. (2016, 5-10 June 2016). *750-nm LED-pumped Nd:YAG laser with 9% optical efficiency.* Paper presented at the 2016 Conference on Lasers and Electro-Optics (CLEO).

Ilev, K. K., Waynant, R. W., Kumagai, H., & Midorikawa, K. (1999). Double-pass fiber Raman laser-a powerful and widely tunable in the ultraviolet, visible, and near-infrared fiber Raman laser for biomedical investigations. *IEEE Journal of*

Selected Topics in Quantum Electronics, 5(4), 1013-1018. doi:10.1109/2944.796324

Jeff, H. (2008). Types of Lasers *Understanding Lasers:An Entry-Level Guide* (pp. 480): Wiley-IEEE Press.

Kanade, V. A. (2017, 20-22 Dec. 2017). *"Organic optical data storage" for securely safeguarding IoT secrets*. Paper presented at the 2017 International Conference on Big Data, IoT and Data Science (BID).

Kekez, M. M. (2018). Laser and Microwave Generations in Nitrogen. *IEEE Transactions on Plasma Science, 46*(3), 545-555. doi:10.1109/TPS.2018.2796304

Kimura, D., Matsubara, S., Otani, K., Ueda, T., Inoue, M., Shimojo, N., . . . Kawato, S. (2013, 12-16 May 2013). *Multimode laser-diode pumped continuous-wave stoichiometric Yb<inf>3</inf>Al<inf>5</inf>O<inf>12</inf> laser*. Paper presented at the 2013 Conference on Lasers & Electro-Optics Europe & International Quantum Electronics Conference CLEO EUROPE/IQEC.

Kopeliovich, D. D. (2014). Gold Alloys. Retrieved from http://www.substech.com/dokuwiki/doku.php?id=gold_alloys

Kotkov, A. A., Budilova, O. V., Ionin, A. A., Kinyaevskiy, I. O., Klimachev, Y. M., & Kozlov, A. Y. (2016, June 27 2016-July 1 2016). *"White light" mid-infrared gas laser systems*. Paper presented at the 2016 International Conference Laser Optics (LO).

Krishna, K. M., & Madhan, M. G. (2016, 6-8 April 2016). *Performance analysis of a low cost VCSEL transmitter based multimode fiber optic link for Gigabit Ethernet application*. Paper presented at the 2016 International Conference on Communication and Signal Processing (ICCSP).

Krokhin, O. (1972). High-temperature laser-produced plasma for controlled nuclear fusion research. *IEEE Journal of Quantum Electronics, 8*(6), 565-565. doi:10.1109/JQE.1972.1077124

Lee, D. (2017). Picosecond IR Pulsed Laser Drilling of Copper-Coated Glass/Epoxy Composite. *IEEE Transactions on Components, Packaging and Manufacturing Technology, 7*(12), 2066-2072. doi:10.1109/TCPMT.2017.2763127

Lee, J., Koo, J., Lee, J., & Lee, J. H. (2016). End-to-End Self-Assembly of Gold Nanorods in Water Solution for Absorption Enhancement at a 1-to-2 micrometer Band for a Broadband Saturable Absorber. *Journal of Lightwave Technology, 34*(22), 5250-5257. doi:10.1109/JLT.2016.2607780

Lee, T. H. (2004). *Planar Microwave Engineering: A Practical Guide to Theory, Measurement, and Circuits*. Stanford University: Cambridge University Press.

Manna, N., & Saha, A. (2011). *Optoelectronics and Optical Communication*. New Delhi: University Science Press.

Miyanaga, N., & Kawanaka, J. (2011, Aug. 28 2011-Sept. 1 2011). *Construction of LFEX PW laser and conceptual design of sub EW laser at Osaka University.* Paper presented at the 2011 International Quantum Electronics Conference (IQEC) and Conference on Lasers and Electro-Optics (CLEO) Pacific Rim incorporating the Australasian Conference on Optics, Lasers and Spectroscopy and the Australian Conference on Optical Fibre Technology.

Monga, K. J. J., Meyer, J., & Manuel, R. M. (2017, 18-20 Sept. 2017). *Implementation of active Q-switching based on a modulated fiber Fabry-Perot filter in linear cavity erbium doped fiber laser.* Paper presented at the 2017 IEEE AFRICON.

Morsin, M. B., Salleh, M. M., & Umar, A. A. (2014, 27-29 Aug. 2014). *Gold nanoplates as sensing material for plasmonic sensor of formic acid.* Paper presented at the 2014 IEEE International Conference on Semiconductor Electronics (ICSE2014).

Ottaway, D. J., Harris, L., Clark, M., & Veitch, P. J. (2016, 5-10 June 2016). *High peak power, short pulse duration Er:YAG lasers using Q-switching and cavity dumping.* Paper presented at the 2016 Conference on Lasers and Electro-Optics (CLEO).

Poprawe, R., Boucke, K., & Hoffman, D. (2018). The History of Laser. In R. Poprawe, K. Boucke, & D. Hoffman (Eds.), *Tailored Light 1: High Power Lasers for Production* (pp. 1-6). Berlin, Heidelberg: Springer Berlin Heidelberg.

Sarri, G. (2015, July 29, 2015). World's most powerful laser is 2,000 trillion watts – but what's it for? Retrieved from http://theconversation.com/worlds-most-powerful-laser-is-2-000-trillion-watts-but-whats-it-for-45891

Shori, R. K., Schepler, K. L., & Clarkson, W. A. (2007). Introduction to the Issue on Progress in Solid-State, Fiber, and Tunable Sources. *IEEE Journal of Selected Topics in Quantum Electronics, 13*(3), 432-434. doi:10.1109/JSTQE.2007.901530

Tan, Y., Chen, F., Aldana, J. R. V. d., Yu, H., & Zhang, H. (2015). QUASI-Three-Level Laser Emissions of Neodymium-Doped Disordered Crystal Waveguides. *IEEE Journal of Selected Topics in Quantum Electronics, 21*(1), 390-394. doi:10.1109/JSTQE.2014.2346613

Tanahashi, I., Manabe, Y., Tohda, T., Sasaki, S., Nakamura, A., D., R., . . . C., F. (1996). Optical nonlinearities of Au/SiO2 composite thin films prepared by a sputtering method. *Journal of Applied Physics, 79*(3), 1244-1249. doi:10.1063/1.361018

Thyagarajan, K., & Ghatak, A. (2010). *Lasers Fundamentals and Applications 2nd Edition* (2nd Edition ed.). New Delhi, India: Springer.

Townes, C. (2004). *Handbook of Laser Technology and Applications* (Vol. 1). London: Institute of Physics Publishing.

Townes, C. H. (1965). 1964 Nobel lecture: Production of coherent radiation by atoms and molecules. *IEEE Spectrum, 2*(8), 30-43. doi:10.1109/MSPEC.1965.6501319

Uchida, S., Agatsuma, S., Hashizu, T., Yamamoto, T., & Ikeda, M. (2006, 11-13 Dec. 2006). *Short wavelength lasers based on GaAs and GaN substrate for DVD and Blu-ray technology.* Paper presented at the 2006 International Electron Devices Meeting.

Ulaby, F. T., Michielssen, E., & Ravaioli, U. (2010). *Fundamentals of Applied Electromagnetics 6/E*: Prentice Hall.

Valster, A., Weegels, L. M., Brouwer, A. A., Corbijn, A. J., Engelen, G. J. P. v., Vermunt, L. W. A., & Lodders, W. H. M. (1998, 4-8 Oct. 1998). *Improved characteristic temperature of 780 nm AlGaAs/AlGaInP QW laser-diodes for high speed laser beam printer applications.* Paper presented at the Conference Digest. ISLC 1998 NARA. 1998 IEEE 16th International Semiconductor Laser Conference (Cat. No. 98CH361130).

Verdeyen, J. T. (1995). *Laser Electronics, Third Edition* (3rd ed.): Prentice Hall.

Wang, J., Xing, Y., Chen, L., Li, S., Jia, H., Zhu, J., & Wei, Z. (2018). Passively Q-Switched Yb-Doped All-Fiber Laser With a Black Phosphorus Saturable Absorber. *Journal of Lightwave Technology, 36*(10), 2010-2016. doi:10.1109/JLT.2018.2800910

Wang, L., Chong, A., & Haus, J. W. (2016, 5-10 June 2016). *Compact, fiber-based Kerr lens saturable absorber.* Paper presented at the 2016 Conference on Lasers and Electro-Optics (CLEO).

Willner, A. E., Byer, R. L., Chang-Hasnain, C. J., Forrest, S. R., Kressel, H., Kogelnik, H., . . . Zervas, M. N. (2012). Optics and Photonics: Key Enabling Technologies. *Proceedings of the IEEE, 100*(Special Centennial Issue), 1604-1643. doi:10.1109/JPROC.2012.2190174

Wu, D., Peng, J., Luo, Z., Weng, J., Cai, Z., & Xu, H. (2017, 7-10 Aug. 2017). *Compact visible Q-switching fiber lasers with transition-metal dichalcogenides.* Paper presented at the 2017 16th International Conference on Optical Communications and Networks (ICOCN).

Wu, H., Song, J., Wu, J., Xu, J., Xiao, H., Leng, J., & Zhou, P. (2018). Concave Gold Bipyramid Saturable Absorber Based 1018 nm Passively Q-Switched Fiber Laser. *IEEE Journal of Selected Topics in Quantum Electronics, 24*(3), 1-6. doi:10.1109/JSTQE.2017.2764068

Wu, K.-H. (Producer). (2009, April 19th, 2018). Lasers: Principles and Applications, Past, Present, and Future. [PowerPoint] Retrieved from https://www.google.com/url?sa=t&rct=j&q=&esrc=s&source=web&cd=5&ved=0ahUKEwi5m-2CqcXaAhXJrI8KHVJfADgQFghLMAQ&url=http%3A%2F%2Fwww.gate.ep.nctu.edu.tw%2Fdownload.php%3Ffilename%3D51_f3113d88.pdf%26dir%3Dusers%2Fresearch%26title%3DDownload&usg=AOvVaw02tS8Gi3zei4buw3cVkbMQ